Праці НТШ
Хім. науки 2018. Т. LIII. С. 7–15

Proc. Shevchenko Sci. Soc.
Chem. Sci. 2018. Vol. LIII. P. 7–15

УДК 546:548.736.4

Volodymyr LEVYTSKYY, Volodymyr BABIZHETSKYY,
Pavlo DEMCHENKO, Bogdan KOTUR

SYSTEM Tb–Ni–C AT 800 °C. CRYSTAL AND ELECTRONIC STRUCTURE OF $TbNiC_2$ SINGLE CRYSTAL

Ivan Franko National University of Lviv,
Kyryla and Mefodiya Str., 6, UA-79005 Lviv, Ukraine
e-mail: v.levyckyy@gmail.com

Phase equilibria at 800 °C in the concentration part up to 33.3 at. % Tb of the Tb–Ni–C system were determined. Three ternary compounds $Tb_{11}Ni_{60}C_6$, $Tb_2Ni_5C_3$ and $TbNiC_2$ have been found to occur at thermodynamically equilibrium conditions. Crystal structure of $TbNiC_2$ was refined by means of a single crystal X-ray diffraction method: structure type $CeNiC_2$, space group Amm2, $a = 3.6010(7)$ Å, $b = 4.5110(9)$ Å, $c = 6.046(1)$ Å, $R1 = 2.2$ %, $wR2 = 5.2$ %. Real-space chemical bonding analysis indicates the $TbNiC_2$ compound represents a unique series of ternary carbide structures stabilized by complex interaction of different types of chemical bonding.

Keywords: phase equilibria, single crystal, crystal structure, chemical bonding.

1. Introduction

Systematic investigation of multicomponent systems is an effective approach to find new compounds. Recently, a high number of new compounds have been discovered when studying the phase equilibria in the systems at a constant temperature. We continue our systematic investigations on the interaction of the components in ternary rare earth (*RE*) – 3*d*-element – carbon systems in respect to their perspectives in developing new functional and energy-effective materials as described in [1]. Due to our recent review [2] we encountered with a contradiction of our results with previously published data concerning Tb–Ni–C system at similar conditions [3]. Therefore, our goal was to clarify the phase equilibria in the Tb–Ni–C system at 800 °C and find reasonable explanation on these uncertainties.

2. Experimental details

More than twenty binary and ternary alloys covering all the phase fields in studied part of the phase diagram have been prepared by arc melting. Commercially available sublimed bulk terbium (Strem Chemicals, 99.9 wt. %), electrolytic nickel (purity of 99.9 wt. %) and graphite rods (Alfa Aesar, 99.999 wt. %) have been used. The samples were homogenized at 800 °C for 30–180 days and afterwards quenched by cold water in evacuated silica ampoules. Experimental data on powder X-ray diffraction (XRD) were obtained by DRON-2.0M diffractometer (Fe*K*α-radiation) for the annealed and cast alloys. Phase analysis was performed using WinCSD [4] and STOE WinXPOW [5] program packages. Additionally, selected samples were mechanically polished and examined by REMMA-102-02 the scanning electron microscope applying energy dispersive X-ray spectroscopy (EDX), where only metal atoms ratio was deduced with quantitative measurement error ±1.5%.

Fine-faced needle-like single crystals of $TbNiC_2$ were separated with a help of a steel non-magnetized needle under optical microscope from a mechanically crushed alloy. Tests for twinning and X-ray diffraction data collection from a suitable single crystal were collected on a STOE IPDS II diffractometer (Mo*K*α-radiation). Single crystal structure determination and refinement was performed using WinGX [6], SHELX [7], and PLATON [8] software.

The Density Functional Theory (DFT) electronic structure calculations were carried out at the basis of experimental structural parameters for $TbNiC_2$ (full unit cell with 8 atoms), with additional optimization (the forces on the atoms are less than 2 mHa/a.u.), using the all-electron full-potential linearized augmented-plane wave code Elk [9], with PBEsol [10] generalized gradient approximation (GGA). For more details concerning procedure of electronic structure calculations and real-space chemical bonding analysis see Ref. [11]. Total energy values in $TbNiC_2$ were converged with accuracy of ~3 meV for the 15×15×15 (960 points) *k*-point mesh in the Brillouin zone. Plane waves have been included up to a cutoff energy of 252.5 eV; electronic states were occupied with a Fermi-Dirac smearing width of 0.027 eV. Real-space chemical bonding in the $TbNiC_2$ was characterized by combining topological analyses of the electron density (ρ) according to quantum theory of atoms in molecules (QTAIM) and the electron localizability indicator (ELI), which was evaluated in the ELI-D representation. Electron density and ELI-D were calculated on an equidistant grid with a mesh size of 0.05 Bohr. All calculations were carried out by the DGrid 4.6e program with Elk support [12, 13] where VESTA [14] and ParaView program packages [15] were used for visualization.

3. Results and discussion

3.1. Phase equilibria

Preliminary results on the Tb–Ni–C system have been presented in [16]. Phase equilibria at 800 °C in the low terbium concentration part of Tb–Ni–C system as a result of present study are shown in Fig. 1a. In comparison with earlier investigation of the system at nearly the same conditions, which results are presented in Fig. 1b [3] we obtained qualitatively different results. First of all, $Tb_2Ni_{22}C_{3-x}$ and $Tb_4Ni_{13}C_4$ ternary compounds reported in [3] have not been confirmed as equilibrium phases in the system at 800 °C. Secondly, new ternary compounds $Tb_{11}Ni_{60}C_6$ and $Tb_2Ni_5C_3$ have been found. As we reported already in [17] both $Tb_2Ni_{22}C_{3-x}$ and $Tb_4Ni_{13}C_4$ phases have been detected in the as cast alloys but were completely decomposed after long term annealing for 180 days at 800 °C yielding a new $Tb_{11}Ni_{60}C_6$ compound as the main phase. This observation provides reason to suggest that the data reported in [3] concern to a non-equilibrium state of the system. Besides, small annealing time for 12–17 d at 797 °C used in [3] supports our conclusion. Similarly to $Tb_{11}Ni_{60}C_6$ compound, another $Tb_2Ni_5C_3$ new ternary phase was observed only in the annealed samples. The results of study of its crystal structure will be reported elsewhere.

No detectable wide homogeneity ranges (> 2 at. %) of binary and ternary phases were observed in the system. The unit cell parameters of the same phases in different phase fields were the same. For comparison, in Table 1 our as well as literature experimental data concerning equilibrium phases, measured at room temperature are summarized.

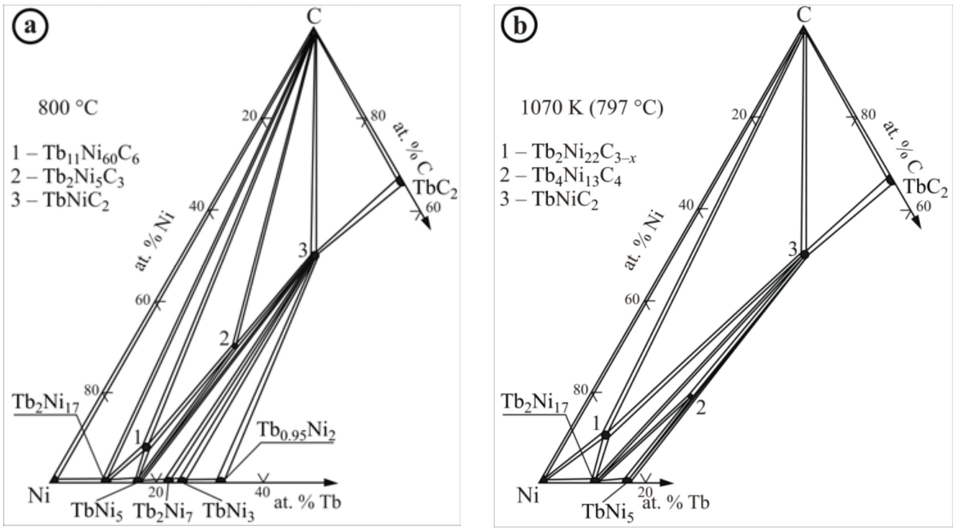

Fig. 1. Phase equilibria at 800 °C in the low terbium concentration part of Tb–Ni–C system: a) results of present study; b) at 797 °C [3].

3.2. Single crystal study of TbNiC$_2$

There are many literature data on the study of crystal and magnetic structure of the TbNiC$_2$ compound using powder diffraction methods (for details, see review [2]). However, every refinement was based on starting atomic parameters of CeNiC$_2$ type structure without taking into account a possible structural peculiarities in TbNiC$_2$ compound itself. This reason we performed a full structural analysis of TbNiC$_2$ single crystal. Preliminary examination of the selected single crystal showed its symmetry belonging to the orthorhombic crystal system with tentative parameters similar to the literature values (however, with interchanged *a* and *c* parameters). Further data collection and their handling with WinGX and WinCSD software confirmed the structure of CeNiC$_2$ type. Finally, it was refined with SHELX-2013 program in anisotropic approximation for metal atoms displacement parameters, whereas only isotropic displacement parameter was refined for carbon atoms site. Details of the single crystal X-ray diffraction data collection and refinement are gathered in Table 2. The refined atomic coordinates and their displacement parameters are shown in Table 3. Crystal structure of TbNiC$_2$ is a distorted AlB$_2$-type structure derivative. Terbium atoms correspond to Al positions whereas Ni atoms and C$_2$-pairs correspond to B positions inside the trigonal prisms. It can be seen from Fig. 2. The C–C distance is δ = 1.36(3) Å, which is close to double C–C bond length value, observed in olefins (δ = 1.34 Å). Other observed interatomic distances lie within the following ranges: $\delta_{\mathrm{Tb–C}}$ = 2.648(13)–2.678(11) Å, $\delta_{\mathrm{Tb–Ni}}$ = 2.958(2)–2.9641(8) Å, and $\delta_{\mathrm{Ni–C}}$ = 1.946(16)–2.000(17) Å.

Table 1

Crystallographic parameters of equilibrium at 800 °C phases of Tb–Ni–C system

Compound	Structure type	Pearson symbol	Space group	Unit cell parameters			V, Å^3	Ref.
				a, Å	b, Å	c, Å		
TbC_2	CaC_2	*tI*6	*I*4/*mmm*	3.6866(3)	–	6.2034(8)	84.31(3)	*
				3.678	–	6.206	83.95	[18]
$TbNi_3$	$PuNi_3$	*hR*36	$R\bar{3}m$	4.9802(5)	–	24.429(6)	524.7(2)	*
				4.967	–	24.46	522.61	[19]
Tb_2Ni_7	β-Gd_2Co_7	*hR*54	$R\bar{3}m$	4.9494(5)	–	36.257(3)	769.2(2)	*
				4.948	–	36.23	768.2	[20]
$TbNi_5$	$CaCu_5$	*hP*6	*P*6/*mmm*	4.9024(4)	–	3.9663(3)	82.55(2)	*
				4.8998	–	3.9599	82.33	[21]
Tb_2Ni_{17}	Th_2Ni_{17}	*hP*38	$P6_3/mmc$	8.316(1)	–	8.044(2)	481.8(2)	*
				8.315	–	8.041	481.5	[22]
$Tb_{11}Ni_{60}C_6$	$Yb_{11}Ni_{60}C_6$	*cI*154	$Im\bar{3}m$	12.50393(6)	–	–	1954.97(3)	[16, 17]*
$Tb_2Ni_5C_3$	$La_2Ni_5C_3$	*tP*20	*P*4/*mbm*	8.2372(1)	–	3.83402(6)	260.14(2)	[16]*
$TbNiC_2$	$CeNiC_2$	*oS*8	*Amm*2	3.6010(7)	4.5110(9)	6.0460(12)	98.21(3)	*
				3.6019	4.5133	6.0570	98.47	[23]

* Our data

Electron localizability indicator (ELI-D, Υ) in the (1 0 0) lattice plane, together with ELI-D isosurface with η_{iso} = 1.39 is shown in Fig. 2. It's clearly seen the main negative charges are localized at C atoms (electron concentration is significantly shifted to non-metal atoms), whereas Tb and Ni atoms remain positively charged. Moreover, there is strong covalent bonding between carbon atoms, which form carbon pairs. Effective atomic charges in $TbNiC_2$ according to QTAIM are $\mathrm{Tb^{+1.48}Ni^{+0.17}(C^{-0.825})_2}$, and the ELI-based oxidation numbers (ELIBON) are $\mathrm{Tb^{2.07+}Ni^{1.75+}(C^{1.91-})_2}$. In Fig. 3 two types of covalent bonding in the $TbNiC_2$ structure are shown. There are two ELI-D disynaptic basins C–C with population 2.49 e^- each (Fig. 3a), indicating a non-polar C–C covalent bonding (intermediate value between single and double bond). Fig. 3b displays C–Ni polar covalent bonding – bond polarity index p(C–Ni) = 0.62 and percentage of electron density ρ(C) = 81.1%. All these results suggest that $TbNiC_2$ structure corresponds to neither typical carbometalate nor intermetallic being an average between carbometalates and intermetallics, which are two large groups of ternary *RE*-containing carbides. Thus, on the $TbNiC_2$ example we concluded on the unique properties of *RE*NiC_2 (*RE* = La→Lu) compounds, which are interesting for further fundamental study of structure-properties correlations.

Table 2

Deatails of data collection and structure refinement of the single crystal of $TbNiC_2$

Refined composition	$TbNiC_2$
Calculated density, g/cm^3	8.172
Absorption coefficient, mm^{-1}	44.79
Number of refined parameters	12
Mode of the refinement	F^2
θ_{min}, θ_{max}, deg.	5.6; 31.7
h, k, l limits	$-5 \leq h \leq 5$,
	$-5 \leq k \leq 6$,
	$-8 \leq l \leq 8$
Number of reflections, all	599
independent	193 ($R_{int} = 0.039$)
Reflections with $I_o \geq 2\sigma(I_o)$	193 ($R_\sigma = 0.030$)
Residuals R_1 (R_1 for all reflections)^a	0,022 (0.022)
wR_2 (wR_2 for all reflections)^b	0,052 (0.052)
S for F^2:	1.055
$\Delta\rho_{min}$ and $\Delta\rho_{max}$ (e·Å^{-3})	–3.49; +1.48

^{a} $R_1 = [\Sigma(|F_o|-|F_c|)]/\Sigma|F_o|$; ^{b} $wR_2 = [\Sigma[w(F_o^2-F_c^2)^2/\Sigma[w(F_o^2)^2]]^{1/2}$;
$w = 1/[\sigma^2(F_o)^2+(0{,}039P)^2]$, where $P = (F_o^2+2F_c^2)/3$

Table 3

Fractional atomic coordinates and their displacement parameters for $TbNiC_2$

Atom	Site	x/a	y/b	z/c	$U_{iso}{}^*/U_{eq}$, Å^2	U_{11}, Å^2	U_{22}, Å^2	U_{33}, Å^2
Tb	2*a*	0	0	0.0000(7)	0.0046(2)	0.0024(3)	0.0062(3)	0.0052(4)
Ni	2*b*	1/2	0	0.6118(5)	0.0056(5)	0.0070(10)	0.0045(11)	0.0053(15)
C	4*e*	0	0.151(3)	0.301(3)	0.009(2)*	–	–	–

$U_{12} = U_{13} = U_{23} = 0$

Conclusions

Phase equilibria at 800 °C in the low terbium concentration part of Tb–Ni–C system have been determined. Present results significantly differ from those reported earlier in [3], which might be explained by a non-equilibrium state of the ternary system. New $Tb_{11}Ni_{60}C_6$ and $Tb_2Ni_5C_3$ phases have been found in the investigated part of phase diagram at the thermodynamically equilibrium conditions. Their synthesis requires a long term homogenization at 800 °C for at least 30 days. Crystal structure of well-known $TbNiC_2$ compound has been determined using single crystal X-ray diffraction data for the first time and its isomorphism with $CeNiC_2$ structure type was confirmed. Real-space chemical bonding analysis of $TbNiC_2$ confirms a unique series of ternary carbide structures *RE*NiC_2 (*RE* = La→Lu) stabilized by complex interaction of different types of chemical bonding.

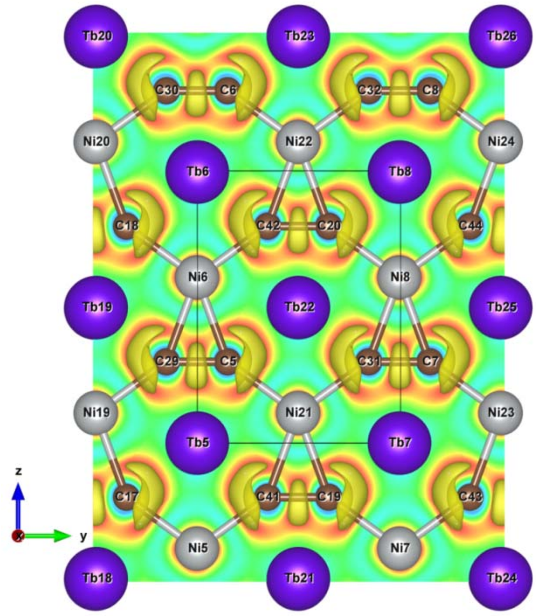

Fig. 2. Electron localizability indicator (ELI-D, ϒ) in the (1 0 0) lattice plane and ELI-D isosurface with $\eta_{iso} = 1.39$ of the crystal structure of $TbNiC_2$.

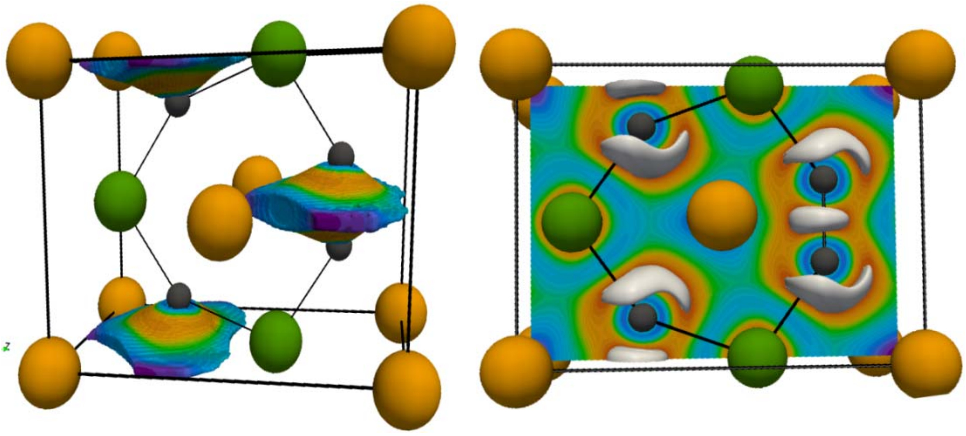

a) **b)**

Fig. 3. Real-space chemical bonding in $TbNiC_2$ structure: a) ELI-D disynaptic basins displaying C–C bonding; b) ELI-D isosurface of $TbNiC_2$ containing carbon and nickel atoms.

Acknowledgement

Electronic structure calculations have been performed with using of Educational Cluster of the Parallel and Distributed Computing at Ivan Franko National University of Lviv. Special thanks to Dr V. Smetana (Stockholm University) for single crystal XRD data collection. Authors are also thankful to reviewer for comments to improve the paper.

LITERATURE

1. *Su D. S., Centi G.* A perspective on carbon materials for future energy application // J. Energy Chem. 2013. Vol. 22. P. 151–173. doi:10.1016/S2095-4956(13)60022-4
2. *Babizhetskyy V., Kotur B., Levytskyy V., Michor H.* Chapter 298: Alloy systems and compounds containing rare earth metals and carbon, in: J.-C.G. Bünzli, V.K. Pecharsky (Eds.), Handbook on the Physics and Chemistry of Rare Earths Including Actinides, Amsterdam: North-Holland, 2017. – pp. 1–263. doi:10.1016/bs.hpcre.2017.09.001
3. *Putyatin A. A.* Interactions in systems Gd (Tb, Dy, Ho)-Ni-C under pressures of 1 atm, 4 and 6 GPa // Izv. Akad. Nauk SSSR. Metally 1991. Vol. 3. P. 204–208. (in Russian). TR: Russ. Metall. 1991. Vol. 3. P. 201–206.
4. *Akselrud L., Grin Y.* WinCSD: software package for crystallographic calculations (Version 4) // J. Appl. Crystallogr. 2014. Vol. 47. P. 803–805. doi:10.1107/S1600576714001058.
5. Stoe WinXPOW (Version 2.1). Stoe & Cie GmbH, Darmstadt, Germany, 2004.
6. *Farrugia L. J.* WinGX and ORTEP for Windows: an update // J. Appl. Crystallogr. 2012. Vol. 45. P. 849–854. doi:10.1107/S0021889812029111
7. *Sheldrick G. M.* A short history of SHELX // Acta Crystallogr. 2008. Vol. A64. P. 112–122. doi:10.1107/S0108767307043930
8. *Spek A. L.* Structure validation in chemical crystallography // Acta Crystallogr. 2009. Vol. D65. P. 148–155. doi:10.1107/S090744490804362X
9. The Elk FP-LAPW Code, available from: http://elk.sourceforge.net
10. *Perdew J. P., Ruzsinszky A., Csonka G. I., Vydrov O. A., Scuseria G. E., Constantin L. A., Zhou X., Burke K.* Restoring the density-gradient expansion for exchange in solids and surfaces // Phys. Rev. Lett. 2008. Vol. 100. P. 136406(1–4). doi:10.1103/PhysRevLett.100.136406
11. *Demchenko P.* Chemical bonding in alumogermanides of erbium and nickel // Visn. Lviv Univ. Series Chem. – 2016. – Is. 57. Pt. 1. – P. 97–104.
12. *Kohout M.* DGrid (Version 4.6), Radebeul, Germany, 2011.
13. *Baranov A. I., Kohout M.* Topological analysis of real space properties for the solid-state full-potential APW DFT method // J. Phys. Chem. Solids 2010. Vol. 71. P. 1350–1356. doi:10.1016/j.jpcs.2010.06.005
14. *Momma K., Izumi F.* VESTA 3 for three-dimensional visualization of crystal, volumetric and morphology data // J. Appl. Crystallogr. 2011. Vol. 44. P. 1272–1276. doi:10.1107/S0021889811038970
15. *Ayachit U.* The ParaView guide: A parallel visualization application // Kitware, 2015, available from: http://www.paraview.org
16. *Levytskyi V., Babizhetskyy V., Kotur B., Demchenko P., Isnard O., Dovgaliuk I.* New compounds in the Tb–Ni–C system // Book Abstr. XXI Internat. Seminar Phys. Chem. Solids (June 10–13, 2018). – Częstochowa, Poland, 2018. – P. 36.

17. *Levytskyi V., Isnard O., Babizhetskyy V., Kotur B.* Synthesis, crystal structure and magnetic properties of $R_{11}Ni_{60}C_6$ (R = Tb, Dy) compounds // J. Phys. Chem. Solids 2018. Vol. 122. P. 189–197. doi:10.1016/j.jpcs.2018.06.010
18. *Atoji M.* Magnetic and crystal structures of CeC_2, PrC_2, NdC_2, TbC_2, and HoC_2 at low temperatures // J. Chem. Phys. 1967. Vol. 46. P. 1891–1901. doi:10.1063/1.1840950
19. *Paccard D., Pauthenet R.* Propriétés cristallographiques et magnétiques des alliages de formule TNi_3, dans laquelle T désigne un métal de terre rare ou l'yttrium // C. R. Seances Acad. Sci., Ser. B. 1967. Vol. 264. P. 1056–1059.
20. *Buschow K. H. J., van der Goot A. S.* The crystal structure of rare-earth nickel compounds of the type R_2Ni_7 // J. Less-Common Met. 1970. Vol. 22. P. 419–428. doi:10.1016/0022-5088(70)90129-3
21. *Vokhmyanin A. P., Lee S., Jang K.-H., Podlesnyak A. A., Keller L., Prokeš K., Sikolenko V. V., Park J.-G., Skryabin Yu. N., Pirogov A. N.* Commensurate–incommensurate phase transition in $TbNi_5$ // J. Magn. Magn. Mater. 2006. Vol. 300. P. e411–e414. doi: 10.1016/j.jmmm.2005.10.179
22. *Buschow K. H. J.* The crystal structures of the rare-earth compounds of the form R_2Ni_{17}, R_2Co_{17} and R_2Fe_{17} // J. Less-Common Met. 1966. Vol. 11. P. 204–208. doi:10.1016/0022-5088(66)90006-3
23. *Jeitschko W., Gerss M. H.* Ternary carbides of the rare earth and iron group metals with $CeCoC_2$- and $CeNiC_2$-type structure // J. Less-Common Met. 1986. Vol. 116. P. 147–157. doi: 10.1016/0022-5088(86)90225-0

РЕЗЮМЕ

Володимир ЛЕВИЦЬКИЙ, Володимир БАБІЖЕЦЬКИЙ, Павло ДЕМЧЕНКО, Богдан КОТУР

СИСТЕМА Tb–Ni–C ПРИ 800 °С. КРИСТАЛІЧНА ТА ЕЛЕКТРОННА СТРУКТУРА МОНОКРИСТАЛА $TbNiC_2$

Львівський національний університет імені Івана Франка,
вул. Кирила і Мефодія, 6, 79005 Львів, Україна
e-mail: v.levyckyy@gmail.com

Для вивчення фазових рівноваг у концентраційній області до 33,3 ат. % Тербію системи Tb–Ni–C методом електродугового сплавляння з чистих компонентів синтезовано більше 20 подвійних та потрійних сплавів. Гомогенізацію зразків проводили у запаяних вакуумованих кварцових ампулах при 800 °С тривалістю 30–180 діб, після чого ампули зі сплавами загартовували у холодній воді. За результатами фазового аналізу, зробленого з використанням методів порошкової рентгенівської дифракції та енергодисперсійної рентгенівської спектроскопії, визначено фазові рівноваги при 800 °С. Виявлено, що рівноважними за таких умов у системі є дві нові тернарних сполуки $Tb_{11}Ni_{60}C_6$, $Tb_2Ni_5C_3$ і відома раніше $TbNiC_2$. Порівняно з давнішими дослідженнями А.А. Путятіна (Изв. АН СССР. Металлы. 1991. № 3. С. 204–208) системи за подібних умов (1070 K ≈ 797 °С) наші результати суттєво відрізняються. Це пояснюється тим, що утворення тернарних сполук, які утворюються в області низького вмісту Тербію, потребує тривалої гомогенізації зразків (не менше 30 діб). Тому, літературні відомості стосовно системи Tb–Ni–C можна вважати такими, що стосуються термодинамічно нерівноважного стану. Підтвердження цього висновку є те, що вказані раніше як рівноважні, сполуки $Tb_2Ni_{22}C_{3-x}$ та $Tb_4Ni_{13}C_4$ ми виявили лише у невідпалених зразках. Виявлені тернарні сполуки при 800 °С не мають помітних областей гомогенності.

Для сполуки $TbNiC_2$ раніше активно вивчалися її фізичні властивості, проте її повне структурне дослідження досі не проводилося. Ми уперше вивчили кристалічну структуру $TbNiC_2$, використавши рентгеноструктурний метод монокристала: структурний тип $CeNiC_2$, просторова група $Amm2$, a = 3,6010(7) Å, b = 4,5110(9) Å, c = 6,046(1) Å, R_1 = 2,2 %, wR_2 = 5,2 %. Уточнено координати атомів та їхні анізотропні (для атомів Тербію та Нікелю) та ізотропні (для атомів Карбону) параметри зміщення при кімнатній температурі. Міжатомні відстані δ_{C-C} = 1,36(3) Å за величиною близькі до довжини подвійного зв'язку C–C в ненасичених вуглеводнях (δ = 1,34 Å). Інші визначені міжатомні відстані лежать в межах наступних інтервалів: $\delta_{\mathrm{Tb–C}}$ = 2,648(13)–2,678(11) Å, $\delta_{\mathrm{Tb–Ni}}$ = 2,958(2)–2,9641(8) Å, $\delta_{\mathrm{Ni–C}}$ = 1,946(16)–2,000(17) Å. Прецизійні структурні параметри атомів з подальшою їхньою оптимізацією використані для квантово-механічних розрахунків з метою аналізу хімічного зв'язку. Ефективні заряди атомів у структурі $TbNiC_2$ згідно QTAIM становлять $\mathrm{Tb}^{+1,48}\mathrm{Ni}^{+0,17}(\mathrm{C}^{-0,825})_2$. Визначені на основі показника локалізації електронів (ELI) ступені окиснення (ELIBON): $\mathrm{Tb}^{2,07+}\mathrm{Ni}^{1,75+}(\mathrm{C}^{1,91-})_2$. Одержані значення додатково підтверджують значний вклад металічного зв'язку у загальний хімічний зв'язок у структурі $TbNiC_2$. Атоми Карбону утворюють пари, зв'язані ковалентним неполярним зв'язком, за кратністю – проміжним між одинарним і подвійним. Між атомами Карбону і атомами Нікелю виявлено полярний ковалентний зв'язок з показником полярності $p_{(\mathrm{C–Ni})}$ = 0,62 та зміщеною електронною густиною до атомів Карбону на $\rho_{(\mathrm{C})}$ = 81,1%. Отримані результати свідчать про те, що сполука $TbNiC_2$ виявляє унікальні електронні властивості, не притаманні типовим комплексним сполукам (карбометалатам) та інтерметалідам. Тому, сполуки ізоструктурного ряду $RENiC_2$ (RE = La→Lu) цікаві для подальших фундаментальних досліджень.

Ключові слова: фазові рівноваги, монокристал, кристалічна структура, хімічний зв'язок.

Стаття надійшла 18.07.2018.
Після доопрацювання 25.08.2018.
Прийнята до друку 28.09.2018.